Supplementary materials

Hydrothermal Synthesis of CuO/RuO$_2$/MWCNT Nanocomposites with Morphological Variants for High Efficient Supercapacitors

Yi-Chen Chung [1,†]**, Ade Julistian** [1,†]**, Lakshmanan Saravanan** [1,2,]*****, Peng-Ren Chen** [1]**, Bai-Cheng Xu** [1]**, Pei-Jie Xie** [1] **and An-Ya Lo** [1,]*****

[1]   Department of Chemical and Materials Engineering, National Chin-Yi University of Technology, Taichung 411030, Taiwan; zxczxazxsbnm@gmail.com (Y.-C.C.); ade.julistian@gmail.com (A.J.); b224466885@gmail.com (P.-R.C.); ples510777@gmail.com (B.-C.X.); eugene1779@gmail.com (P.-J.X.)

[2]   Department of Micro and Nanoelectronics, Saveetha School of Engineering, Saveetha Institute of Medical and Technical Sciences (SIMATS), Thandalam 602105, Tamil Nadu, India

*****   Correspondence: ljsaravanan08@gmail.com (L.S.); aylo@ncut.edu.tw (A.-Y.L.)

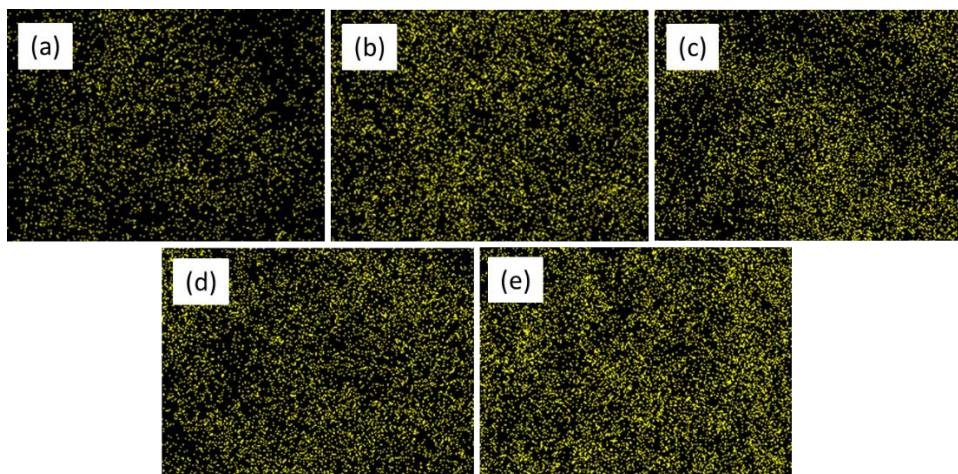[†]   These authors contributed equally to this work.

Figure S1. EDS-Mapping images of $C_{35}R_yM$ electrodes with (a)11, (b) 16, (c) 17, (d) 20, and (e) 23 wt% Ru.
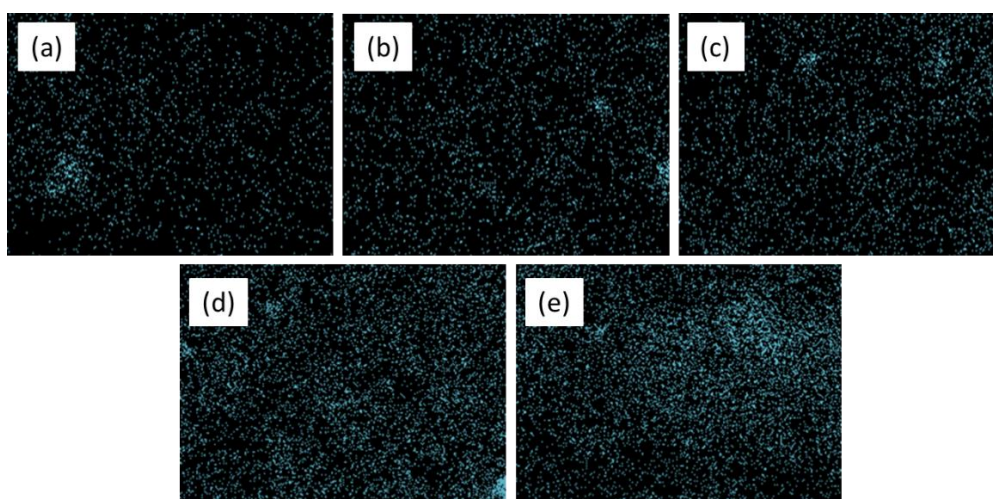

Figure S2. EDS mapping of $C_xR_{20}M$ electrodes with (a) 7, (b) 8, (c) 9, (d) 10, and (e) 11 wt% Cu.
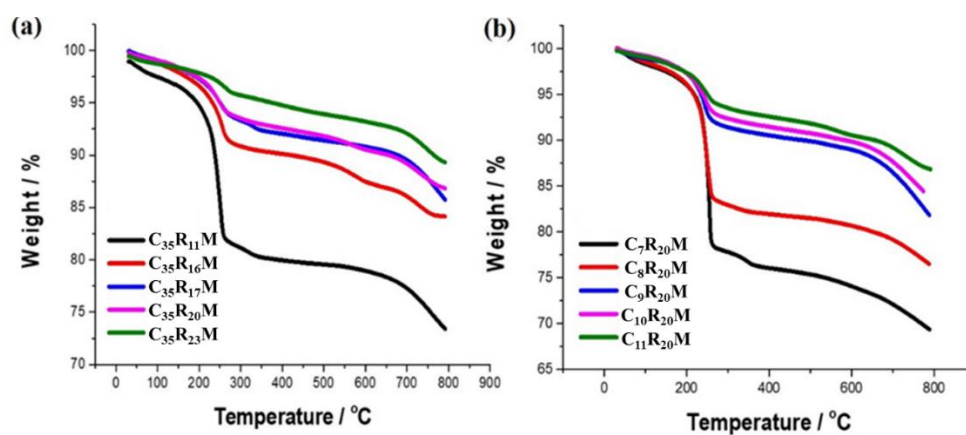

Figure S3. The TGA curves of (a) the $C_{35}R_yM$ nanocomposites with various content of Ru and (b) the $C_xR_{20}M$ nanocomposites with various content of Cu.

Table S1. The residual weight percentage and thermal stability of the $C_{35}R_yM$ nanocomposites with various content of Ru.

Specimen Designation	Ru content (%)	The residual weight %	Thermal stability (°C)
$C_{35}R_{11}M$	11	73.40	755.24
$C_{35}R_{16}M$	16	84.14	728.11
$C_{35}R_{17}M$	17	85.73	785.70
$C_{35}R_{20}M$	20	86.83	734.05
$C_{35}R_{23}M$	23	89.32	744.43

Table S2. The residual weight percentage and thermal stability of the $C_xR_{20}M$ nanocomposites with various content of Cu.

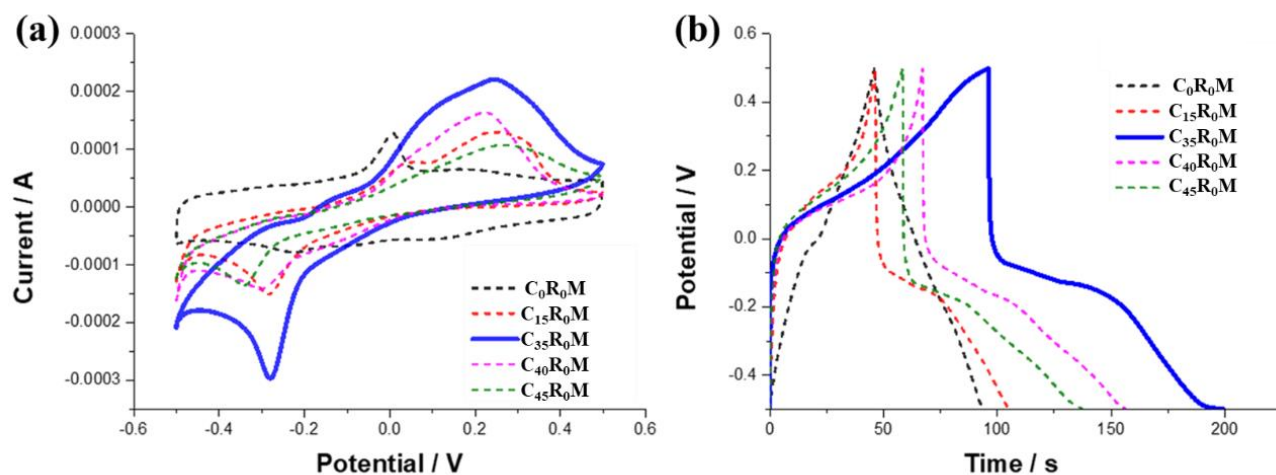| Specimen Designation	Ru content (%)	The residual weight %	Thermal stability (°C)
$C_7R_{20}M$	7	63.71	735.27
$C_8R_{20}M$	8	73.89	784.31
$C_9R_{20}M$	9	78.66	752.01
$C_{10}R_{20}M$	10	81.42	744.32
$C_{11}R_{20}M$	11	86.83	734.12

Figure S4. (a) CV curves of C_xR_0M electrodes with various Ru content, at a scan rate of 10 mVs^{-1}, (b) GCD curves of C_xR_0M electrodes with various Ru content, at a current density of 1 Ag^{-1}.

Table S3. The specific capacitance of the C_xR_0M electrodes valuated by CV curves and GCD curves, with various content of Cu.

Specimen Designation	Cu content (%)	Specific Capacitance (F/g) by CV curves	Specific Capacitance (F/g) by GCD curves
C_0R_0M	0	45.31	46.80
$C_{15}R_0M$	15	51.92	58.40
$C_{35}R_0M$	35	104.71	103.50
$C_{40}R_0M$	40	61.75	89.20
$C_{45}R_0M$	45	52.10	78.70

Table S4. Comparison of electrochemical properties of $CuO/RuO_2/MWCNT$ with samples reported in literature.

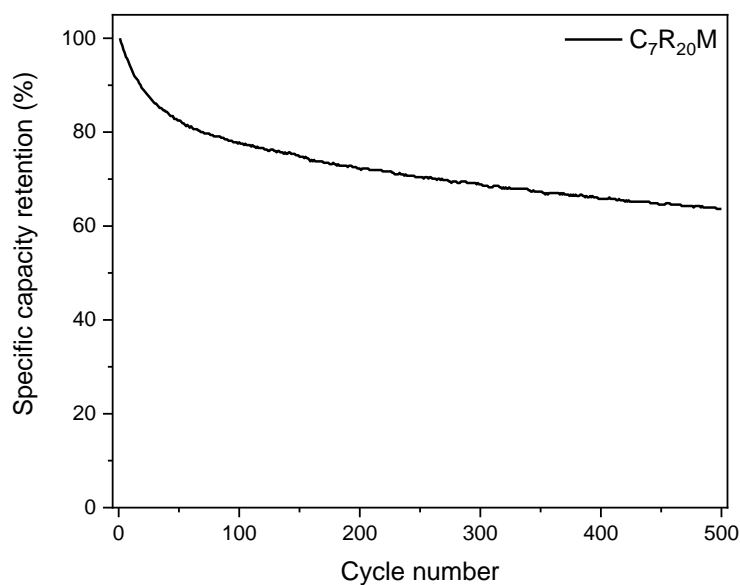| Composite	Electrolyte	Specific capacitances	Current densities	[Ref.]
CuO/NTs	1 M $LiPF_6$	150 F /g	1 A/ g	[36]
g-C_3N_4/CuO	4 M KOH	95 F /g	1 A/ g	[37]
CuONPs/ MWCNTs	0.5 M Na_2SO_4	221.66 F/g	10 mV	[38]
RuO_2-CNTS-CC	1 M H_2SO_4	171.3 F/ g	10 mA/cm_2	[39]
RuO_2/MWNT	3 M KCl	16.94 mF/cm_2	0.2 mA/cm_2	[19]
$CuCo_2O_4$/ CuO@RuO_2-2// AC	10 mM $RuCl_3$	454.3 F /g	10 mA /cm_2	[40]
CuO/RuO_2/ MWCNT	3 M $(NH_4)_2SO_4$	461.59 F/g	1 A/g	This work

Figure S5. Cyclic stability test of $C_7R_{20}M$ electrode.